Avoiding chromosome pathology when replication forks collide

Christian J. Rudolph, Amy L. Upton, Anna Stockum, Conrad A. Nieduszynski and Robert G. Lloyd

Supplementary Information

SUPPLEMENTARY TABLES AND FIGURES

Table S1. *Escherichia coli* K-12 strains

Strain	Relevant Genotype [a]	Source [c]
(a) General P1 donors		
CGSC7488	*zji-202::*Tn*10*	CGSC[d]
JJC256	*hsdR ΔtusA::kan*	[32]
JC19257	*ΔpriC303::kan ΔpriB202 dnaA809,820*	[33]
KL227	Hfr *metB1 relA1 λ–*	[34]
RUC663	*tnaA::*Tn*10 dnaA46*	Tove Atlung
(b) AB1157 and derivatives [b]		
AB1157	*rec*$^+$	[34]
AM2123	*ΔrecG::apra*	AB1157 × P1.AM1655 to Apra^r
N3695	*ΔrecG263::kan srgA1*	[35]
N3793	*ΔrecG263::kan*	[36]
N4441	*ΔrecG263::kan metB1 argE*$^+$	N3793 × P1.KL227 to Arg$^+$
N5494	*Δtus::kan*	AB1157 × P1.JJC256 to Km^r
WX296	*oriZ-cat*	[17]
RCe455	*oriZ-cat ΔrecG::apra*	WX296 × P1.AM1655 to Apra^r
(c) MG1655 and derivatives [b]		
MG1655	F$^-$ *rph-1*	[34]
AM1581	*ΔlacIZYA recB268::*Tn*10*	[37]
AM1655	*ΔrecG::apra*	[37]
AM1672	*ΔrecD::dhfr*	[37]
AM1675	*ΔrecB::dhfr*	A.A. Mahdi and RGL, unpublished
AM1775	*Δtus::cat*	A.A. Mahdi and RGL, unpublished
AM2013	*ΔpriB::dhfr*	[38]

AM2017	*ΔlacIZYA ΔpriB::dhfr*	[38]
AM2018	*ΔlacIZYA ΔrecG::apra ΔpriB::dhfr*	[38]
AM2129	*rpoB*35 ΔrecG::apra*	[38]
AS1056	*rpoB*35 ΔrecG::apra Δtus::cat ΔoriC::kan*	RCe261 × P1.RCe395
AU1053	*ΔlacIZYA tnaA::*Tn*10 dnaA46*	TB28 × RUC633 to Tc^r
AU1054	*tnaA::*Tn*10 dnaA46*	MG1655 × P1.RUC663 to Tc^r
AU1057	*ΔlacIZYA tnaA::*Tn*10 dnaA46* pAU101e	AU1053 × pAU101[e] to Ap^r
AU1059	*ΔlacIZYA tnaA::*Tn*10 dnaA46 rnhA::cat* pAU101[e]	AU1057 × P1.N4704 to Cm^r
AU1066	*ΔlacIZYA tnaA::*Tn*10 dnaA46 rnhA::cat*	plasmid-free derivative of AU1059
AU1091	*tnaA::*Tn*10 dnaA46 ΔrecG263::kan*	AU1054 × P1.N3793 to Kan^r
AU1218	*recG[wt]-kan[a]*	ALU and RGL, unpublished
JJ1119	*ΔlacIZYA ΔrecG::apra* pJJ100	[39]
JJ1257	*ΔlacIZYA argE86::Tn10*	TB28 × P1.N4837 to Tc^r Arg^-
JJ1261	*ΔlacIZYA metB1*	JJ1257 × N4441 to Arg^+ Met^-
JJ1264	*ΔlacIZYA srgA1*	JJ1261 × P1.N3695 to Met^+
JJ1268	*ΔlacIZYA srgA1 ΔrecG::apra*	JJ1264 × P1.AM1655 to $Apra^r$
JJ1359	*ΔlacIZYA dam1::kan ΔrecG::apra tus1::dhfr*	J. Zhang and RGL, unpublished
JJ1378	*ΔlacIZYA tus1::dhfr*	TB28 × P1-JJ1359 to Tm^r
MGK297	*att*Tn*7::tetO240-gen zdd/e::lacO240-cat tos-kan*	[16]
N4235	*ΔrelA251::kan ΔspoT207::cat rpoB*35*	[37]
N4560	*recG265::cat*	[40]
N4702	*ΔrecG263::kan recB268::*Tn*10*	[41]
N4704	*rnhA::cat*	[15]
N4837	*argE86::*Tn*10*	[37]
N4849	*rpoB*35*	[37]
N5535	*rpoB*35 priA300*	[37]
N5933	*priA300 ΔlacIZYA* pAM374	[37]
N6071	*priA300 ΔlacIZYA ΔrecG::apra* pAM374	N5933 × P1.AM1655 to $Apra^r$
N6424	*ΔpriC303::kan ΔpriB202 dnaA809,820 zji-202::*Tn*10*	[38]
N6537	*ΔlacIZYA ΔrecG::apra*	[38]
N6576	*ΔlacIZYA ΔrecG::apra*	[39]
N6796	*tus1::dhfr*	MG1655 × P1.JJ1359 to Tm^r
N6859	*priA300 ΔlacIZYA ΔrecG::apra*	plasmid-free derivative of N6071
N6953	*ΔxonA::apra ΔxseA::dhfr ΔsbcCD::kan*	[15]
N7957	*ΔrecG::apra Δtus::cat*	AM1655 × P1.AM1775 to Cm^r
N8191	*ΔlacIZYA srgA1 ΔrecG::apra argE86::Tn10*	JJ1268 × P1.N4837 to Tc^r Arg^-
N8192	*ΔlacIZYA srgA1 ΔrecG::apra rpoB*35*	N8191 × P1.N4235 to Arg^+
N8196	*ΔlacIZYA rpoB*35 ΔrecG::apra Δtus::cat ΔpriB::dhfr*	RCe261 × P1.AM2017 to Tm^r
N8199	*ΔlacIZYA srgA1 ΔrecG::apra rpoB*35 Δtus::cat*	N8192 × P1.AM1775 to Cm^r
N8201	*rpoB*35 ΔrecG::apra Δtus::cat tnaA::*Tn*10 dnaA46*	RCe268 × P1.N6424 to Km^r

	ΔpriC303::kan	
N8205	*ΔlacIZYA rpoB*35 ΔrecG::apra Δtus::cat ΔpriB::dhfr tnaA::*Tn*10 dnaA46*	N8196 × P1.AU1053 to Tc^r
N8206	*ΔlacIZYA srgA1 ΔrecG::apra rpoB*35 Δtus::cat tnaA::*Tn*10 dnaA46*	N8199 × P1.AU1053 to Tc^r
N8226	*ΔrecG::apra*	MG1655 × P1.AM1655 to $Apra^r$
N8227	*Δtus::cat*	MG1655 × P1.AM1775 to Cm^r
RCe203	*tnaA::*Tn*10 dnaA46 Δtus::kan*	AU1054 × P1.N5494 to Km^r
RCe205	*tnaA::*Tn*10 dnaA46 Δtus::kan ΔrecG::apra*	RCe203 × P1.AM1655 to $Apra^r$
RCe260	*rpoB*35 Δtus::cat*	N4849 × P1.AM1775 to Cm^r
RCe261	*rpoB*35 ΔrecG::apra Δtus::cat*	AM2129 × P1.AM1775 to Cm^r
RCe262	*rpoB*35 tnaA::*Tn*10 dnaA46*	N4849 × P1.RUC663 to Tc^r
RCe263	*rpoB*35 ΔrecG::apra tnaA::*Tn*10 dnaA46*	AM2129 × P1.RUC663 to Tc^r
RCe267	*rpoB*35 Δtus::cat tnaA::*Tn*10 dnaA46*	RCe260 × P1.RUC663 to Tc^r
RCe268	*rpoB*35 ΔrecG::apra Δtus::cat tnaA::*Tn*10 dnaA46*	RCe261 × P1.RUC663 to Tc^r
RCe302	*rpoB*35 priA300 ΔrecG::apra*	N5535 × P1.AM1655 to $Apra^r$
RCe303	*rpoB*35 tnaA::*Tn*10 dnaA46 rnhA::cat*	RCe262 × P1.N4704 to Cm^r
RCe306	*rpoB*35 priA300 ΔrecG::apra Δtus::cat*	RCe302 × P1.AM1775 to Cm^r
RCe309	*rpoB*35 tnaA::*Tn*10 dnaA46 rnhA::cat tus1::dhfr*	RCe303 × P1.N6796 to Tm^r
RCe313	*rpoB*35 priA300 ΔrecG::apra Δtus::cat tnaA::*Tn*10 dnaA46*	RCe306 × P1.RUC663 to Tc^r
RCe331	*rpoB*35 Δtus::cat tnaA::*Tn*10 dnaA46 recG^{wt}-kan*[a]	RCe268 × P1.AU1218 to Km^r ($Apra^s$)
RCe364	*rpoB*35 Δtus::cat tnaA::*Tn*10 dnaA46 ΔrecG::apra*	RCe331 × P1.RCe205 to $Apra^r$ (Km^s)
RCe381	*rnhA::cat ΔoriC::kan*[a]	this study; derived from N4704 *via* single step gene disruption[27]
RCe383	*ΔlacIZYA tnaA::*Tn*10 dnaA46 rnhA::cat* N15 lysogen	AU1066 × N15 to $N15^r$
RCe384	*rpoB*35 ΔrecG::apra Δtus::cat tnaA::*Tn*10 dnaA46* N15 lysogen	RCe268 × N15 to $N15^r$
RCe385	*rpoB*35 ΔrecG::apra Δtus::cat tnaA::*Tn*10 dnaA46 tos-kan*	RCe268 × P1.MGK297 to Km^r
RCe387	*rpoB*35 ΔrecG::apra Δtus::cat tnaA::*Tn*10 dnaA46 tos-kan* N15 lysogen	RCe385 × N15 to $N15^r$
RCe391	*recG265::cat tos-kan*	N4560 × P1.MGK297 to Km^r
RCe393	*rpoB*35 ΔrecG::apra Δtus::cat tnaA::*Tn*10 dnaA46 ΔoriC::kan*[a]	This study, derived from RCe268 *via* single step gene disruption[27]
RCe395	*rpoB*35 tnaA::*Tn*10 dnaA46 rnhA::cat tus1::dhfr ΔoriC::kan*[a]	This study, derived from RCe309 *via* single step gene disruption[27]
RCe399	*recG265::cat tos-kan* N15 lysogen	RCe391 × N15 to $N15^r$
RCe401	*ΔlacIZYA tnaA::*Tn*10 dnaA46 rnhA::cat tos-kan*	AU1066 × P1.MGK297 to Km^r
RCe404	*ΔlacIZYA tnaA::*Tn*10 dnaA46 rnhA::cat tos-kan* N15 lysogen	RCe401 × N15 to $N15^r$

RCe405	*tnaA::*Tn*10 dnaA46 recG263::kan* N15 lysogen	AU1091 × N15 to N15^r
RCe409	*recG265::cat tos-kan tnaA::*Tn*10 dnaA46*	RCe391 × P1.RUC663 to Tc^r
RCe418	*recG265::cat tos-kan tnaA::*Tn*10 dnaA46* N15 lysogen	RCe409 × N15 to N15^r
RCe427	*tos-kan*	MG1655 × P1.MGK297 to Km^r
RCe429	*tos-kan* N15 lysogen	RCe427 × N15 to N15^r
RCe435	*rpoB*35 ΔrecG::apra Δtus::cat tnaA::*Tn*10 dnaA46 recB::dhfr – transductant A*	RCe268 × P1.AM1675 to Tm^r
RCe436	*rpoB*35 ΔrecG::apra Δtus::cat tnaA::*Tn*10 dnaA46 recB::dhfr – transductant B*	RCe268 × P1.AM1675 to Tm^r
RCe437	*rpoB*35 ΔrecG::apra Δtus::cat tnaA::*Tn*10 dnaA46 recD::dhfr – transductant A*	RCe268 × P1.AM1672 to Tm^r
RCe438	*rpoB*35 ΔrecG::apra Δtus::cat tnaA::*Tn*10 dnaA46 recD::dhfr – transductant B*	RCe268 × P1.AM1672 to Tm^r
RCe446	*tnaA::*Tn*10 dnaA46 ΔrecG263::kan recB::dhfr*	AU1091 × P1.AM1675 to Tm^r
TB28	*ΔlacIZYA<>frt*	[42]

[a] The abbreviations *kan, cat, dhfr* and *apra* refer to insertions conferring resistance to kanamycin (Km^r), chloramphenicol (Cm^r), trimethoprim (Tm^r) and apramycin (Apra^r), respectively. Tn*10* confers resistance to tetracycline (Tc^r). Plasmids carry an ampicillin (Amp^r) resistance marker. Strains carrying *dnaA46* are temperature sensitive for growth. *recG^{wt}-kan* refers to the wild type *recG* sequence followed immediately by a kanamycin resistance cassette, thereby allowing replacement of mutant *recG* alleles with a wild type copy. *ΔoriC* refers to a replacement of the entire origin region (754 bp) including DnaA boxes and 13mers as well as the entire *mioC* gene by a kanamycin resistance cassette (see Fig. S1). *tos-kan* refers to the telomerase occupancy site from the bacteriophage N15 genome followed by a kanamycin resistance cassette[16].

[b] Only the relevant additional genotype of the derivatives is shown.

[c] The term "× N15 to N15^r" refers to isolation of *E. coli* cells lysogenized with bacteriophage N15. These cells can be identified by their resistance to re-infection with N15 (see Supplementary Material and Methods).

[d] Coli Genetic Stock Center, Yale University.

[e] Plasmid pJJ100, pAM374, pAM375 and pAM490 have been described elsewhere[15,37]. All three carry *lac$^+$*. In addition, pJJ100 carries *recG$^+$*, pAM374 carries *priA$^+$*, pAM375 carries *recB$^+$* and pAM490 carries *rnhA$^+$*. pAU101 is a derivative of pRC7 carrying the coding sequence for *dnaA$^+$* including its native promoter, which was PCR amplified from MG1655 using 5' and 3' primers incorporating *Apa*I sites. The PCR product was cloned into the *Apa*I site within *lacI^q* to give pAU101. The coding sequence inserted is transcribed in the same orientation as the disrupted *lacI^q* gene. pAU101 complements the temperature sensitivity of the *dnaA46* strain AU1054.

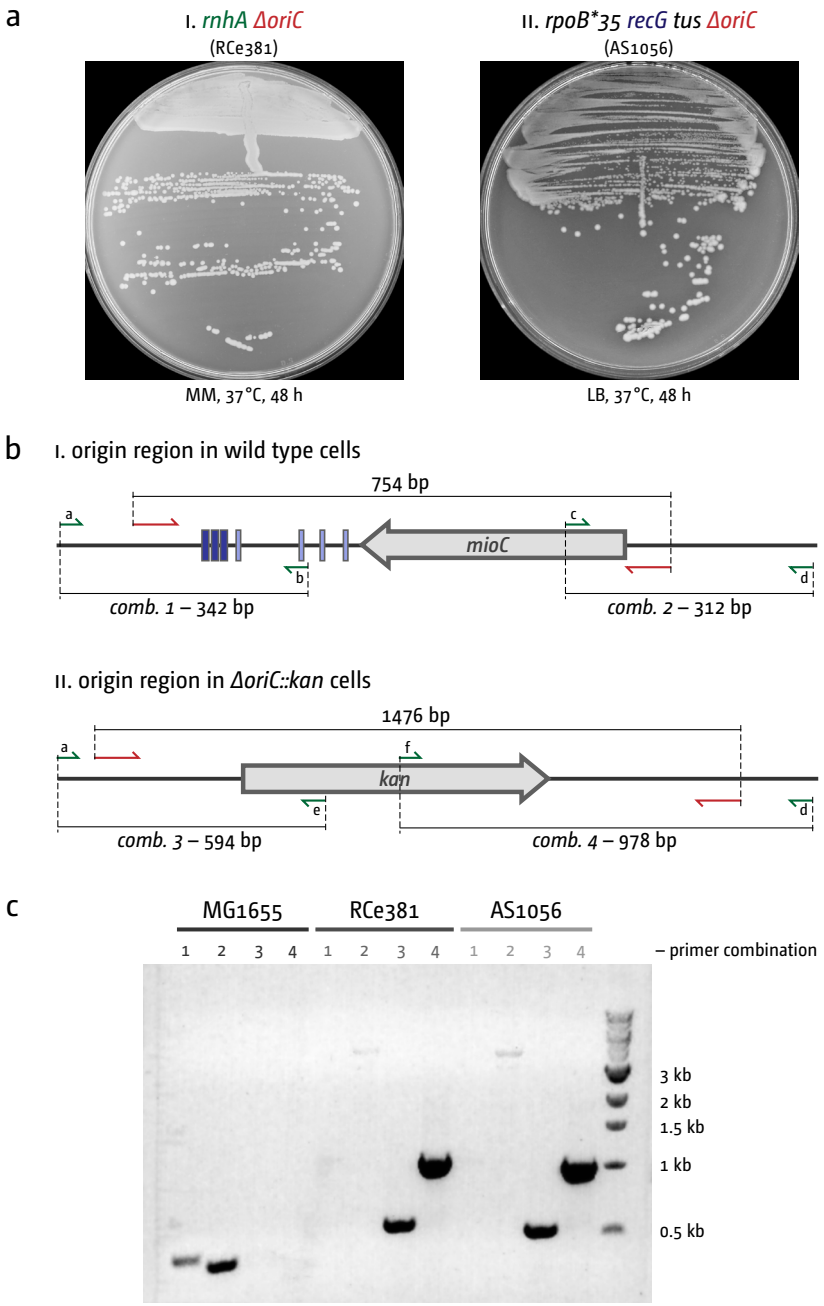

Supplementary Figure 1. Deletion of *oriC* in cells lacking RNase HI or RecG helicase. **(a)** Growth of *ΔrnhA* (RCe381) and a *ΔrecG Δtus rpoB*35* (AS1056) cells deleted for *oriC* on minimal and LB agar, respectively. The origin region was removed by using the single-step gene replacement method[27]. **(b)** Schematic representation of the origin region before and after the disruption event. The approximate position of the 40 bp homology tails used for the disruption are shown in red (length of the primers is not to scale). Primers used for verification of the deletion are shown in green (a – f). The sizes of the PCR products are indicated between the appropriate primer combinations. **(c)** PCR verification of the *oriC::kan* deletion. All strains were tested using 4 primer combinations, thereby testing for the presence or absence of the wild type region as well as the replacement cassette as indicated in b. In wild type cells only primer combinations a/b and c/d generate a PCR product. In the deletion mutants only primer combinations a/e and d/f generate a PCR product, verifying that the wild type origin region has been exchanged for the kanamycin resistance cassette.

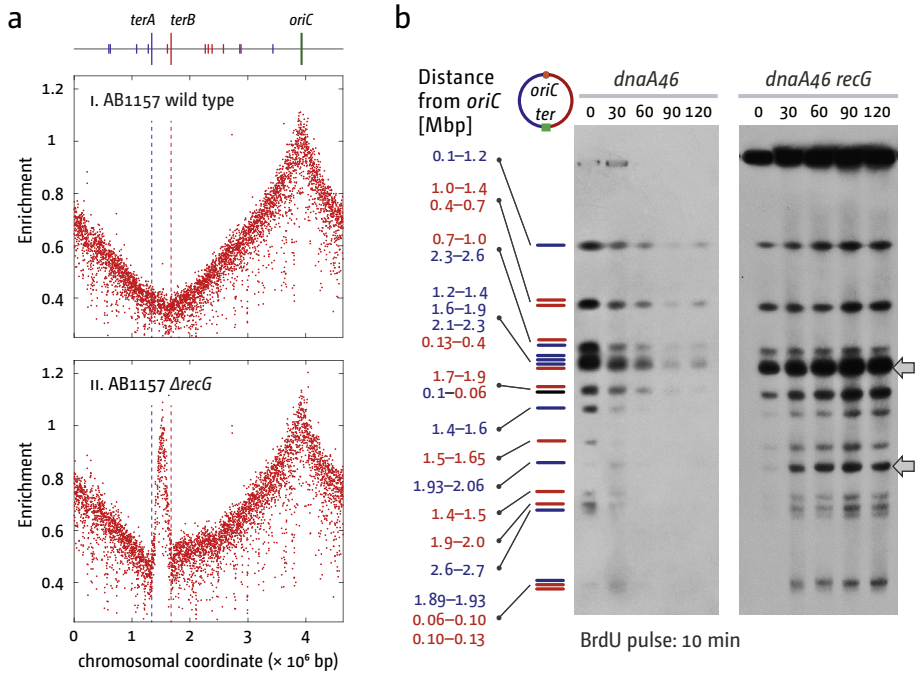

Supplementary Figure 2. Origin independent synthesis in cells lacking RecG helicase. **(a)** AB1157 *ΔrecG* cells show over-amplification of the termination area, as shown by marker frequency analysis of the *E. coli* chromosome. The normalised number of reads (logarithmically versus stationary cultures) is plotted against the chromosomal location. Sequencing templates were isolated from AB1157 and AM2123 (AB1157 *ΔrecG*). All cultures were grown at 37°C. **(b)** BrdU pulse labelling of *dnaA46* and *dnaA46 ΔrecG* cells following DnaA inactivation by shift to 42 °C. Cultures of *dnaA46* strains of the genotypes indicated were pulse labelled with BrdU as described (Material and Methods). While active synthesis runs out in *recG*$^{+}$ cells, ongoing synthesis is observed in the absence of RecG helicase. Synthesis is particularly strong within the termination area (fragments indicated by an arrow). A schematic *Not*I restriction pattern of the *E. coli* chromosome is shown on the left. The distance from *oriC* to each end of the fragments is indicated. Fragments clockwise and anticlockwise of *oriC* are shown in red and blue, respectively; the fragment containing *oriC* is shown in black. The strains used were AU1054 (*dnaA46*) and AU1091 (*dnaA46 ΔrecG*). The images have been reproduced from [49].

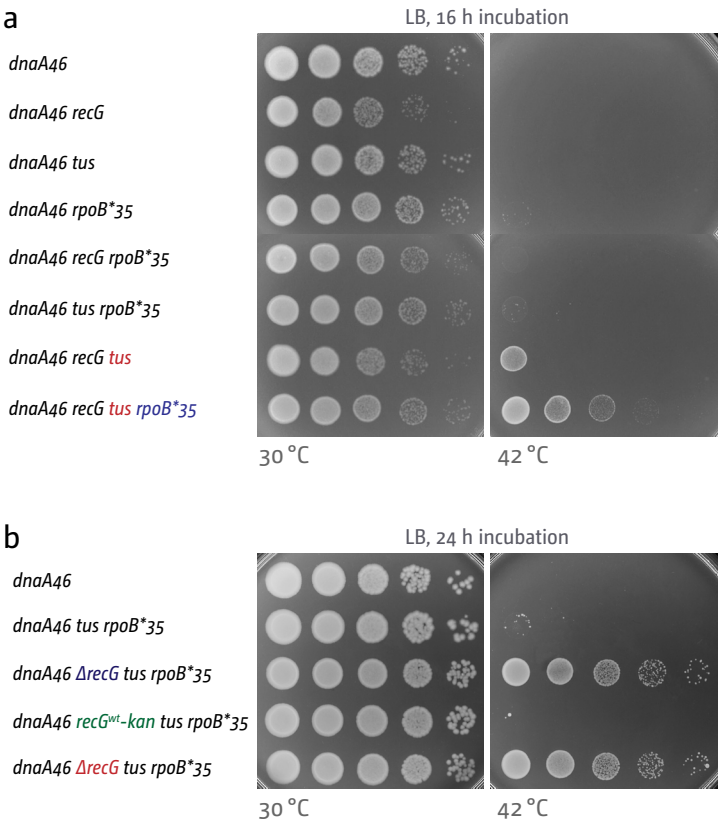

Supplementary Figure 3. Effect of Tus, RNA polymerase and PriA mutations on growth and DNA synthesis of *dnaA46 ΔrecG* strains. **(a)** Spot dilution assay showing the effect of *Δtus* and *rpoB*35*. The strains used were AU1054 (*dnaA46*), AU1091 (*dnaA46 ΔrecG*), RCe203 (*dnaA46 Δtus*), RCe262 (*dnaA46 rpoB*35*), RCe263 (*dnaA46 ΔrecG rpoB*35*), RCe267 (*dnaA46 Δtus rpoB*35*) RCe205 (*dnaA46 ΔrecG Δtus*) and RCe268 (*dnaA46 ΔrecG Δtus rpoB*35*). **(b)** Growth of *dnaA46 ΔrecG Δtus rpoB*35* cells in the absence of origin firing is not caused by a background mutation. If the *ΔrecG::apra* allele is replaced with the *recG* wild type sequence linked to a kanamycin marker (*recG*^{wt}*-kan*) growth is suppressed. If *ΔrecG* is re-introduced *via* P1*vir* transduction, the ability of cells to grow at restrictive temperature is restored. The strains used were AU1054 (*dnaA46*), RCe205 (*dnaA46 Δtus rpoB*35*), RCe268 (*dnaA46 ΔrecG Δtus rpoB*35*), RCe331 (*dnaA46 recG*^{wt}*-kan Δtus rpoB*35*) and RCe364 (*dnaA46 ΔrecG Δtus rpoB*35*).

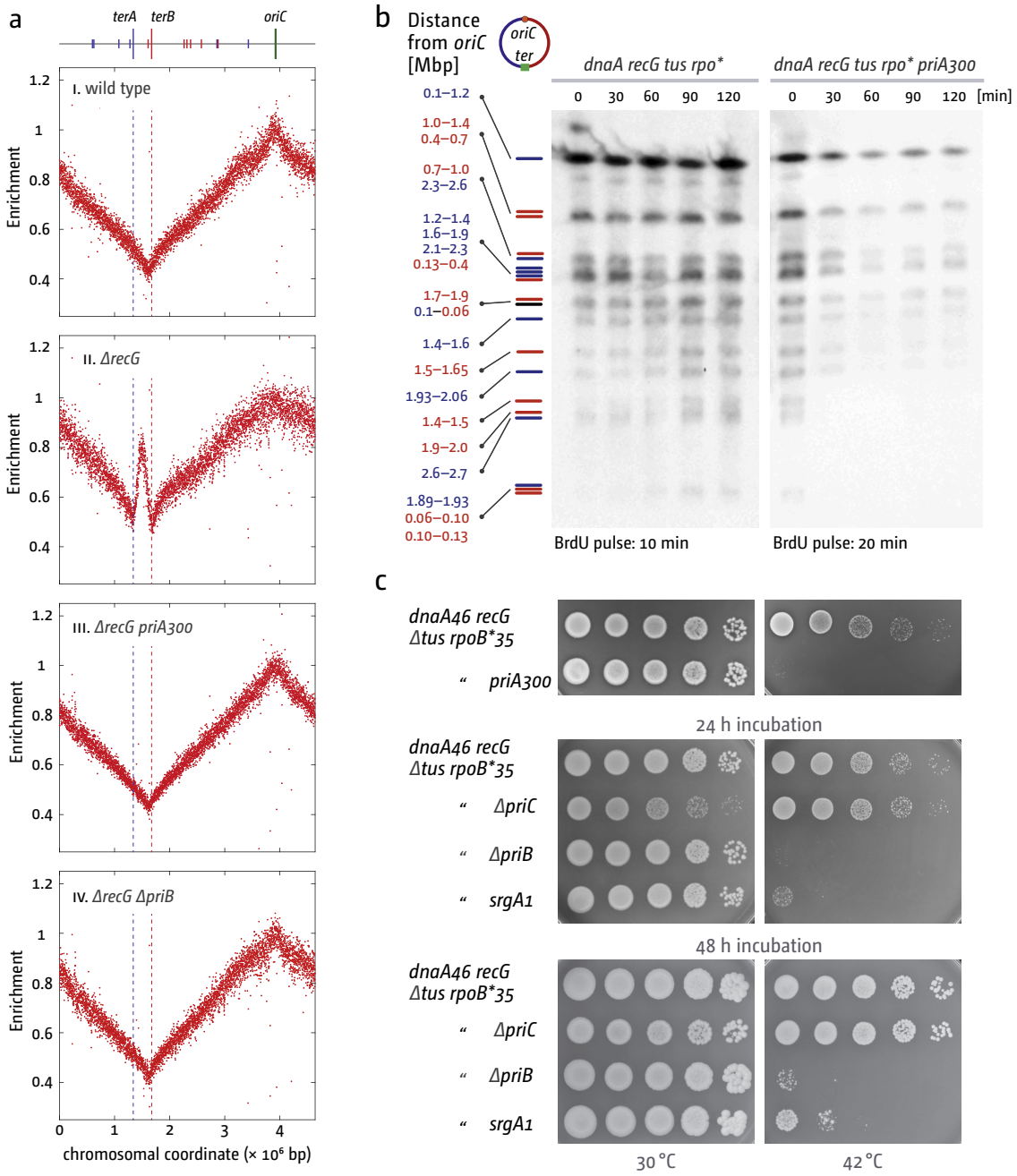

Supplementary Figure 4. Effect of restart protein PriA on origin-independent synthesis of cells lacking RecG. **(a)** Marker frequency analysis of *E. coli ΔrecG* harbouring a point mutation in *priA* which inactivates the helicase activity (*priA300*) or a *priB* deletion. The normalised number of reads (logarithmically versus a stationary wild type culture) is plotted against the chromosomal location. Sequencing templates were isolated from MG1655, N6859 (*ΔrecG priA300*) and AM2018 (*ΔrecG ΔpriB*). Data for *ΔrecG* were reproduced from Fig. 2 for comparison. **(b)** BrdU pulse labelling of *dnaA46 ΔrecG Δtus rpoB*35* in the presence and absence of PriA helicase activity. The cultures were pulse labelled with BrdU essentially as described (Material and Methods). However, due to the low levels of synthesis in the *priA300* construct the pulses were extended to 20 min (in contrast to the 10 min pulse used for *dnaA46 ΔrecG Δtus rpoB*35* cells). A schematic *Not*I restriction pattern of the *E. coli* chromosome is shown on the left. The distance from *oriC* to each end of the fragments is indicated. Fragments clockwise and anti-clockwise of *oriC* are shown in red and blue, respectively; the fragment containing *oriC* is shown in black. The strains used were RCe268 (*dnaA46 ΔrecG Δtus rpoB*35*) and RCe313 (*dnaA46 ΔrecG Δtus rpoB*35 priA300*). **(c)** Spot dilution assays for growth without DnaA. The strains used were RCe268 (*dnaA46 recG tus rpoB*35*), RCe313 (*dnaA46 recG tus rpoB*35 priA300*), N8201 (*dnaA46 recG tus rpoB*35 priC*), N8205 (*dnaA46 recG tus rpoB*35 priB*) and N8206 (*dnaA46 recG tus rpoB*35 srgA1*).

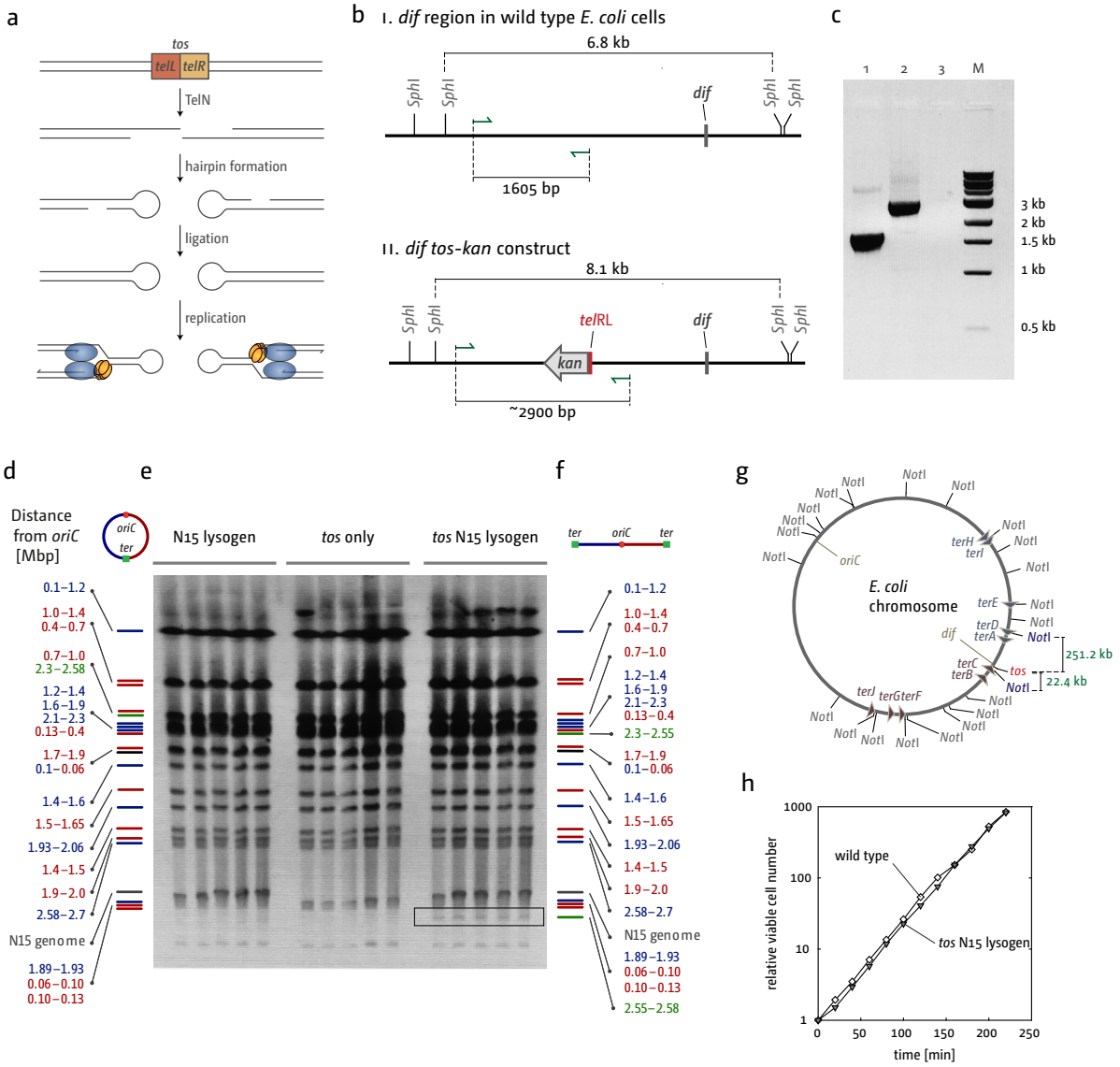

Supplementary Figure 5. Linearisation of the *E. coli* chromosome. **(a)** Schematic indicating how *tos* is processed by the bacteriophage N15 telomerase, TelN, and how the resulting hairpin generation prevents the collision of replication forks. Segregation of the chromosomes depends on replication of the entire hairpin. This results in the generation of a chromosomal dimer and simultaneously in the restoration of the two *tos* sites which are immediately cleaved and processed by TelN, resulting in the generation of two separate linear chromosomes that can be segregated[16]. **(b)** Schematic representation of the area around *dif* with and without integrated *tos-kan* site. The linearisation verification primers are shown in green (for primer sequences see [16]) and the PCR product sizes in wild type cells and integrants are indicated. **(c)** PCR products generated with the linearisation verification primers for wild type cells lysogenized with phage N15 (lane 1), *tos-kan* cells and *tos-kan* cells lysogenized with phage N15 (lane 3). The shift of the PCR product size in a non-linearised strain as shown in lane 2 indicates the presence of the *tos-kan* cassette. Linearisation of the chromosome (lane 3) prevents formation of a PCR product since the chromosome is cleaved between the primer binding sites. **(d–g)** Verification of chromosome linearisation by pulse field gel electrophoresis. A negative image is shown for clarity. If the *tos* site is cleaved by TelN an additional band becomes visible on the gels. The *tos* site is located in the 273.6 kb *Not*I fragment between positions 1 337 601 and 1 611 219 (c, highlighted in green) and cleavage by TelN splits it into two fragments, one of which is 251.2 kb and the other one 22.4 kb (e and f, highlighted in green). The 251.2 kb fragment moves into the quadruplet around 250 kb and thus is hidden in between other fragments **(f)**. The smaller 22.4 kb fragment, however, becomes visible as an additional fragment at the bottom of the gel highlighted by a black rectangle (d and e). **(h)** Linearisation of the chromosome does not delay growth of wild type cells. The strains used were MG1655 and RCe363 (*tos* N15 lysogen).

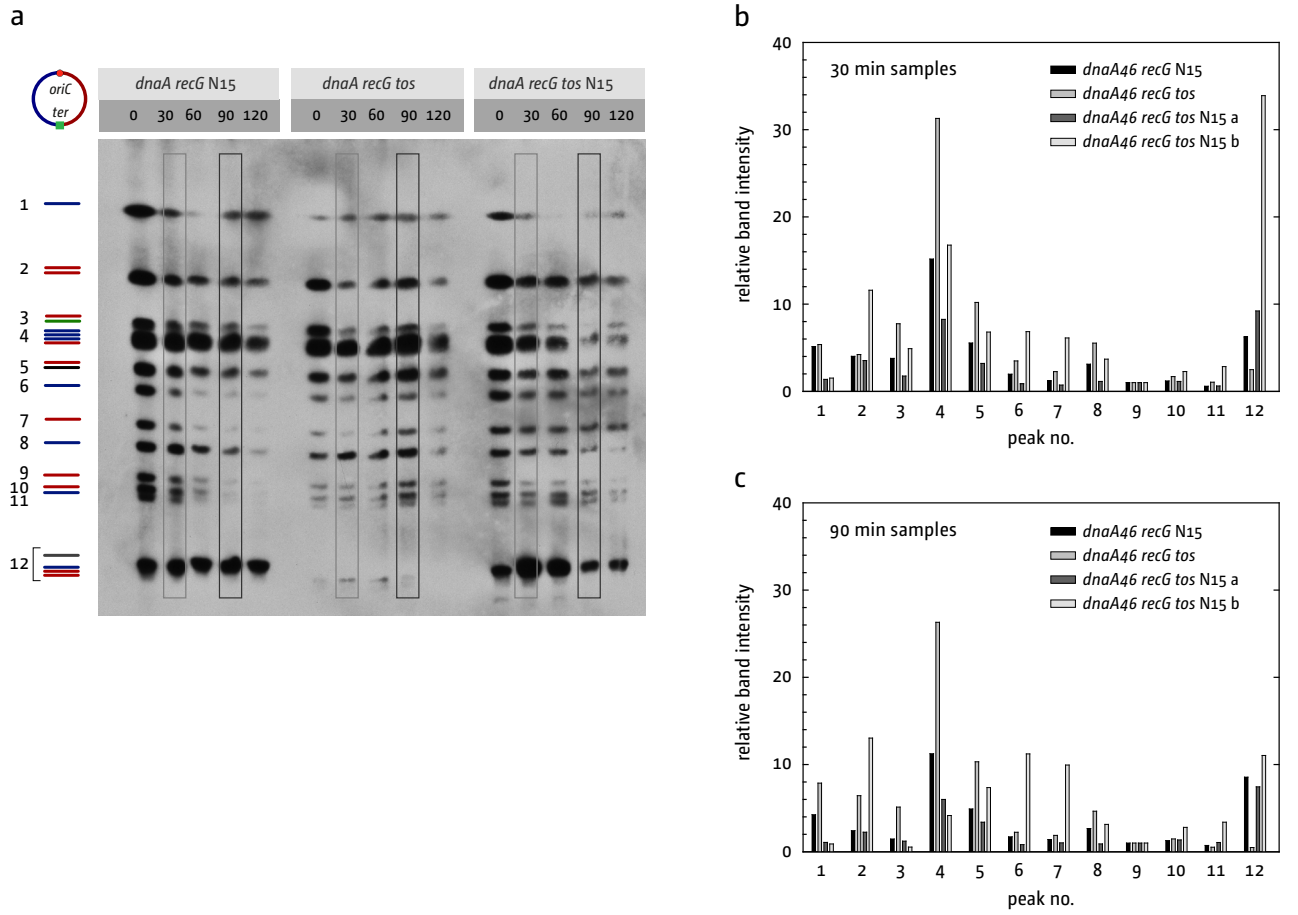

Supplementary Figure 6. Effect of chromosome linearisation on DnaA-independent growth and terminus amplification. **(a)** Fluorograph of BrdU incroporation in cells with a linearised chromosome as well as control constructs. Strains used were RCe405 (*dnaA46 ΔrecG* N15 lysogen), RCe409 (*dnaA46 ΔrecG tos*) and RCe418 (*dnaA46 ΔrecG tos* N15 lysogen). The rectangles indicate the lanes used for the analysis of band intensities shown in panels b and c. (**b–c**) Semi-quantitative analysis of band intensities of the lanes indicated in panel a. Quantifiable bands were numbered as shown in panel a. Signal intensities of bands for each strain were measured relative to band no. 9, which is a clearly defined, non-saturated single fragment band. The set of data labelled b shows values from a second, independent experiment. The data sets show that for both controls the signal intensity of band 8, which is located in the terminus area, is higher than the signal intensity of band 7, whereas, following linearisation, the signal intensity of band 8 is either similar or reduced in comparison to band 7. Furthermore, linearisation leads to a reduction of the signal intensity of the quadruplet (band 4), especially 90 min following shift to restrictive temperature.

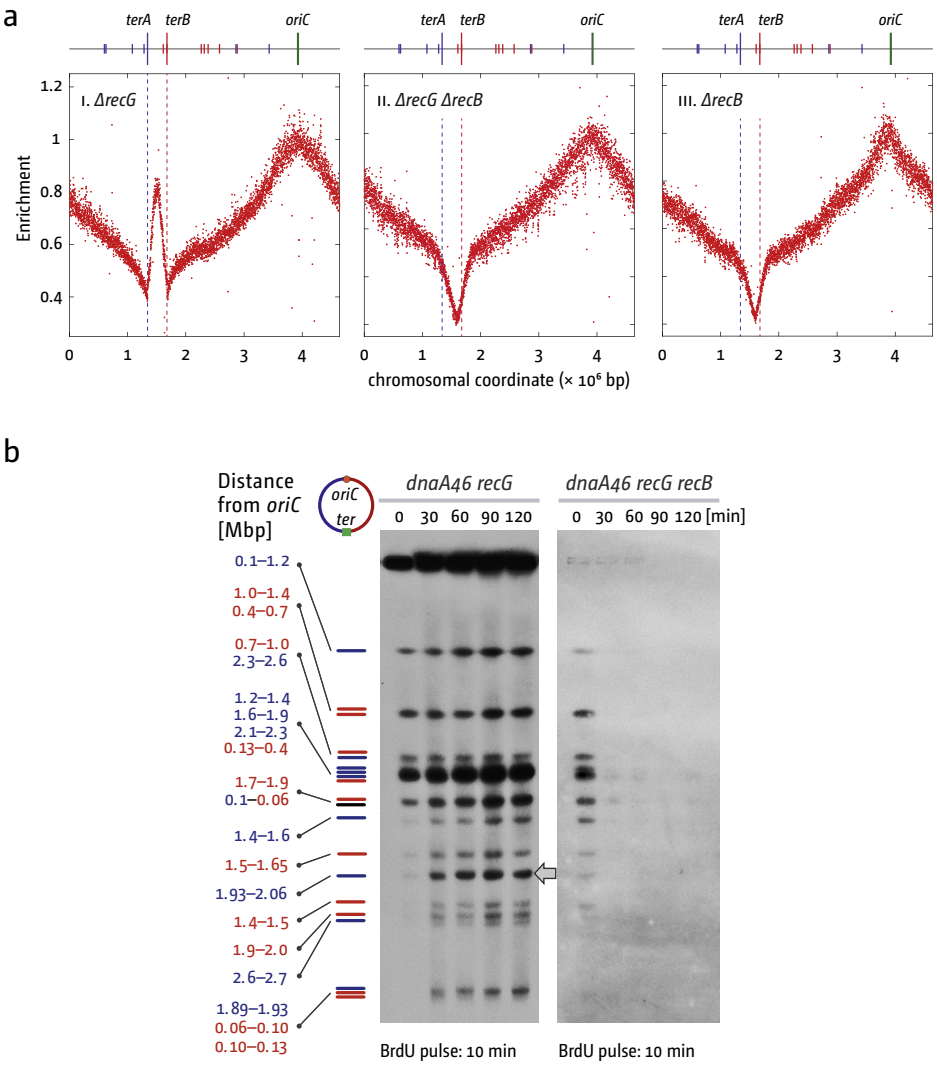

Supplementary Figure 7. Effect of RecB inactivation on origin-independent synthesis of cells lacking RecG. **(a)** Marker frequency analysis of the chromosome in exponential phase cells. The sequencing template was isolated from strain (*recB*) cultured at 37°C. The data for *recG* and *recG recB* were reproduced from Fig. 3c for comparison. **(b)** Cultures of the strains indicated were pulse labelled with BrdU as described (Material and Methods). While active synthesis does not run out in *ΔrecG* cells, ongoing synthesis disappears in the absence of RecB recombinase activity. A schematic *Not*I restriction pattern of the *E. coli* chromosome is shown on the left. The distance from *oriC* to each end of the fragments is indicated. Fragments clockwise and anti-clockwise of *oriC* are shown in red and blue, respectively; the fragment containing *oriC* is shown in black. The strain used was RCe446 (*dnaA46 ΔrecG ΔrecB*). The image for *dnaA46 ΔrecG* has been reproduced from [49] (see Supplementary Figure 2b).

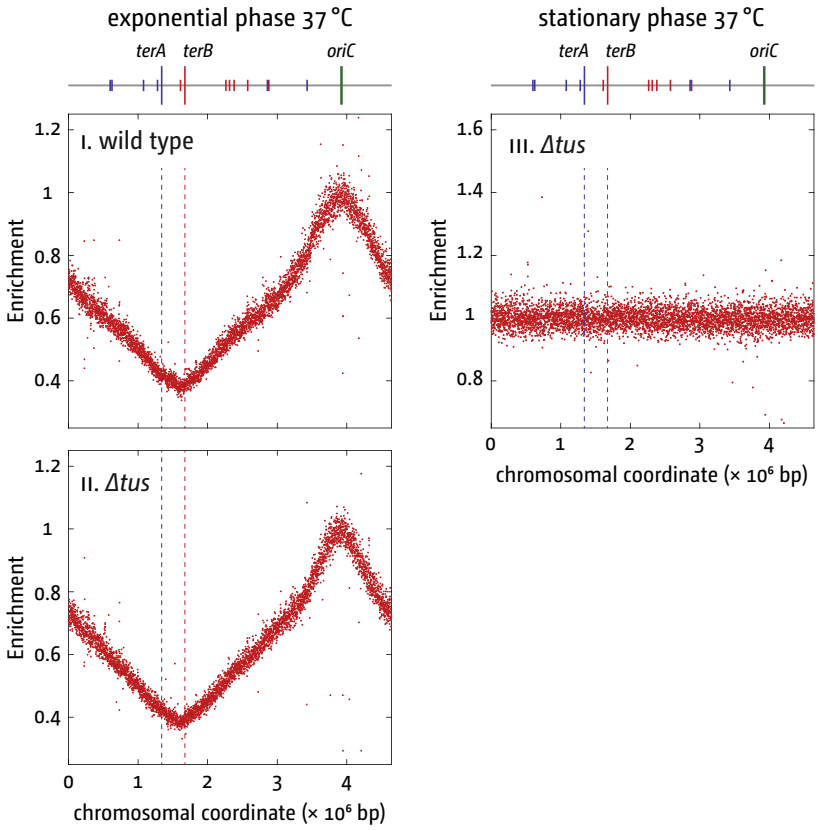

Supplementary Figure 8. Marker frequency analysis of the chromosome of *tus* cells in exponential *vs* stationary phase cells grown at 37 °C. For stationary phase cells, sequencing templates were isolated after prolonged incubation of cultures with vigorous aeration until well after no further increase in cell density was detectable. The strains used were MG1655 (wild type) and N8227 (*tus*). Data for logarithmically growing tus cells were reproduced from Fig. 4a for comparison.

SUPPLEMENTARY DISCUSSION

Events associated with the collision of two replication forks

The idea that when two replisome complexes meet one fork might displace the nascent leading strand of the opposing fork, thereby generating a 3' flap, was stimulated by an earlier report demonstrating over-replication of an *oriC* plasmid when replisome complexes assembled at *oriC* were allowed to collide[43]. Because formation of a 3' flap is not observed with DnaB alone[44], it was suggested that nascent leading strand displacement is a particular risk following collision between fully-fledged replisomes[3], an idea supported by *in vivo* observations[45,46]. DnaB would most likely collide with and dislodge the leading strand polymerase of the opposing fork to which the 3' end of the nascent leading strand is engaged (Fig. 3a). Displacement would generate a 3' ssDNA flap, which is a substrate for 3' exonucleases, RecG or PriA helicase. Given that the affinity of RecG for 3' flaps is 10-fold higher than that of PriA[47] the 3' flap is likely to be degraded directly by 3' single-stranded exonucleases or converted by RecG to a 5' flap and subsequently degraded by 5' single-stranded exonucleases. We predict that in the absence of RecG or 3' ssDNA exonucleases this 3' ssDNA flap persists for longer, thereby providing a substrate that PriA could exploit to trigger assembly of a new replication fork. As this fork progresses it would generate a duplex arm with a free DNA end, which, if processed by RecBCD, may then invade the re-replicated DNA behind the fork (or the sister duplex) via RecA recombinases (Fig. 3a)[15,3,48,49], forming a D-loop. This D-loop is another substrate for PriA to establish yet another fork moving in the opposite direction.

Displacement of the 3' leading strands by DnaB might explain why we observed some over-replication of sequences in the terminus area in a *recG* derivative of a strain that has had its chromosome linearised by the N15 telomere generating system (Fig. 2d). This synthesis is only observed if forks coming from *oriC* reach the hairpin. In *dnaA46 recG tos* strains in which the chromosome is linearised due to N15 lysogenisation the level of BrdU incorporation in the termination area is reduced below the level of a distant control fragment if *oriC* firing is inhibited by a shift to 42°C (Fig. 2c and Supplementary Fig. 6). This strongly suggests that the synthesis observed in the terminus area is the result of the forks established at *oriC* moving through the hairpin. Translocation of DnaB through the hairpin at the chromosome end means that it would move on to what had been the leading strand template up to that point (Supplementary Fig. 5a), creating a situation similar to that proposed to occur following the collision of converging forks (Fig. 3a). Some displacement of the nascent leading strand might then trigger initiation of replication, thus accounting for the residual amplification of sequences corresponding to the normal terminus area (Fig. 2d, panel iii). However, and regardless of whether a 3' flap was displaced, translocation of DnaB through the hairpin and the continuation of replication would itself lead to some re-replication of the already replicated DNA until a Tus/*ter* site was reached.

Termination in cells with two replication origins

The amplification of sequences spanning the *terA–terB* interval in *ΔrecG* cells containing a duplication of *oriC* (Fig. 3e) is remarkable, as the peak exceeds that at either origin, as if this region is duplicated when other regions of the chromosome are not. The same is true for cells lacking 3' ssDNA

exonuclease activity of Exonuclease I, Exonuclease VII or SbcCD, even though the amplification is not as substantial (Fig. 2a). An amplification of the terminus area above the level of *oriC* might be explained if the initiation events titrated out essential replication proteins in a significant fraction of the cells, preventing further firing of either copy of the origin and thus leading to over-replication of the terminus region. However, it is also important to note that potentially two forks initiated as consequence of the collision event will travel until they reach the first non-permissive *ter*/Tus complex, where progression will be blocked. Therefore, subsequent two forks coming from *oriC* will each collide with a fork arrested at *ter*/Tus. This will result in multiple over-replication events in the terminus area which might contribute to the high marker frequency. Furthermore, it also might be no coincidence that the fork held up at *terC* will have duplicated the *dif* locus some time before the arrival of the opposing fork from *oriC*. Xer-*dif* recombination mediated before the chromosome is fully duplicated might have pathological consequences that trigger some initiation of replication at this position, at least in the absence of RecG.

SUPPLEMENTARY REFERENCES

32 Bierne, H., Ehrlich, S. D. & Michel, B. Deletions at stalled replication forks occur by two different pathways. *EMBO J.* **16**, 3332–3340 (1997).

33 Sandler, S. J. et al. dnaC mutations suppress defects in DNA replication- and recombination-associated functions in *priB* and *priC* double mutants in *Escherichia coli* K-12. *Mol. Microbiol.* **34**, 91–101 (1999).

34 Bachmann, B. J. in *Escherichia coli and Salmonella*. Cellular and Molecular Biology, (Second Edition) eds F.C. Neidhardt et al.) 2460–2488 (ASM Press, 1996).

35 Al-Deib, A. A., Mahdi, A. A. & Lloyd, R. G. Modulation of recombination and DNA repair by the RecG and PriA helicases of *Escherichia coli* K-12. *J. Bact.* **178**, 6782–6789 (1996).

36 Mahdi, A. A., Sharples, G. J., Mandal, T. N. & Lloyd, R. G. Holliday junction resolvases encoded by homologous *rusA* genes in *Escherichia coli* K-12 and phage 82. *J. Mol. Biol.* **257**, 561–573 (1996).

37 Mahdi, A. A., Buckman, C., Harris, L. & Lloyd, R. G. Rep and PriA helicase activities prevent RecA from provoking unnecessary recombination during replication fork repair. *Genes Dev.* **20**, 2135–2147 (2006).

38 Mahdi, A. A., Briggs, G. S. & Lloyd, R. G. Modulation of DNA damage tolerance in *Escherichia coli recG* and *ruv* strains by mutations affecting PriB, the ribosome and RNA polymerase. *Mol. Microbiol.* **86**, 675–691 (2012).

39 Zhang, J., Mahdi, A. A., Briggs, G. S. & Lloyd, R. G. Promoting and avoiding recombination: contrasting activities of the *Escherichia coli* RuvABC Holliday junction resolvase and RecG DNA translocase. *Genetics* **185**, 23–37 (2010).

40 Meddows, T. R., Savory, A. P. & Lloyd, R. G. RecG helicase promotes DNA double-strand break repair. *Mol. Microbiol.* **52**, 119–132 (2004).

41 Bolt, E. L. & Lloyd, R. G. Substrate specificity of RusA resolvase reveals the DNA structures targeted by RuvAB and RecG *in vivo*. *Mol. Cell* **10**, 187–198 (2002).

42 Bernhardt, T. G. & de Boer, P. A. The *Escherichia coli* amidase AmiC is a periplasmic septal ring component exported *via* the twin-arginine transport pathway. *Mol. Microbiol.* **48**, 1171–1182 (2003).

43 Hiasa, H. & Marians, K. J. Tus prevents overreplication of *oriC* plasmid DNA. *J. Biol. Chem.* **269**, 26959–26968 (1994).

44 Kaplan, D. L. & O'Donnell, M. DnaB drives DNA branch migration and dislodges proteins while encircling two DNA strands. *Mol. Cell* **10**, 647–657 (2002).

45 Markovitz, A. A new *in vivo* termination function for DNA polymerase I of *Escherichia coli* K12. *Mol. Microbiol.* **55**, 1867–1882 (2005).

46 Krabbe, M., Zabielski, J., Bernander, R. & Nordström, K. Inactivation of the replication-termination system affects the replication mode and causes unstable maintenance of plasmid R1. *Mol. Microbiol.* **24**, 723–735 (1997).

47 Tanaka, T. & Masai, H. Stabilization of a stalled replication fork by concerted actions of two helicases. *J. Biol. Chem.* **281**, 3484–3493 (2006).

48 Rudolph, C. J., Upton, A. L., Harris, L. & Lloyd, R. G. Pathological replication in cells lacking RecG DNA translocase. *Mol. Microbiol.* **73**, 352–366 (2009).

49 Rudolph, C. J., Upton, A. L., & Lloyd, R. G. Replication fork collisions cause pathological chromosomal amplification in cells lacking RecG DNA translocase. *Mol. Microbiol.* **74**, 940–955 (2009).